RSC Advances

PAPER

View Article Online
View Journal | View Issue

Cite this: *RSC Adv.*, 2023, **13**, 7585

Polyimide/crown ether composite film with low dielectric constant and low dielectric loss for high signal transmission†

Heming Li,[a] Xinming Wang,[a] Yuze Gong,[ab] Hongbin Zhao,[ac] Zhaobin Liu,[c] Lin Tao,[a] Youyou Peng,[d] Ke Ma,*[a] Zhizhi Hu*[ac] and Davoud Dastan*[e]

Dielectric properties of polyimide (PI) are constrained by its inherent molecular structure and inter-chain packing capacities. The compromised dielectric properties of PI, however, could be rescued by introducing trifluoromethyl and forming a host–guest inclusion complex with the introduction of crown ethers (CEs). Herein, we report PI/crown ether composite films as a communication substrate that could be applied under high frequency circumstances. In this work, three kinds of bisphenol A-containing diamine (2,2′-bis[4-(4-aminophenoxy)phenyl]propane, 2,2-bis[4-(2-methyl-4-aminophenoxy)phenyl] propane, and 2,2-bis[4-(2-trifluoro methyl-4-aminophenoxy)phenyl]propane) are synthesized and polymerized with 4,4′-(hexafluoroisopropylidene)diphthalic anhydride to prepare low-dielectric PI films by means of thermal imidization. Crown ethers are introduced into the PI with different mass fractions to obtain three series of PI films. Following the combination of trifluoromethyl into the molecular chain of PI, high frequency dielectric loss of modified PI films can be effectively reduced. The properties of these materials (especially the dielectric properties) are thoroughly explored by crown ether addition. The results show that the crown ether addition process can offer crown ethers with increased free volume of PI matrix, thus allowing them to generate a special necklace-like supramolecular structure, which makes the crown ether disperse more uniformly in the PI matrix, resulting in improved dielectric properties. Importantly, the dielectric constant and dielectric loss of the composite films at high frequencies are remarkably reduced to 2.33 and 0.00337, respectively. Therefore, these composite films are expected to find extensive use as a 5G communication substrate at high frequencies in the future.

Received 6th November 2022
Accepted 21st February 2023

DOI: 10.1039/d2ra07043j

rsc.li/rsc-advances

1. Introduction

The progress of information transmission technology towards high-frequency microwaves and highly integrated electronic devices has been the thought route of the current communication technology.[1] With the manufacturing technique development of high frequency communication, 5G communications have transmitted at the speeds of nearly 10 gigabits and have delayed by less than 1 ms.[2,3] However, the wide range of user access and the decay speed of the transmitted signal cause an increased demand for low-dielectric constant materials. In order to achieve high fidelity and low delay characteristics of high-frequency signal transmission, a substitute with low dielectric constant (D_k) and low dielectric loss factor (D_f) is urgently needed to take the place of traditional silica materials.[4–6] Polyimide (PI) is generally rated as a suitable candidate due to its low molecular polarizability and outstanding thermal, mechanical, and chemical resistance characteristics and exhibits desirable prospects in the electronic and microelectronic industries.[7] Currently, the structure and composition design of low-dielectric polymer materials mainly focus on structural modification, improvement of the material manufacture process, and composite modification. The inherent dielectric constant of conventional PIs lies at approximately 3.5, however, a lower value is usually required to minimize the power dissipation and delay of signal transmission in inter-layer dielectrics for ultra-large-scale integrated circuits, high frequency communication antenna substrate, and millimeter wave radar.[8–11] Many methods have been studied to reduce the dielectric constant and the dielectric loss of PIs by decreasing the polarization between imide groups on the main chains.[12] The molecular structure of the PI polymer plays a major role in its dielectric properties. The combination of the orientation polarization of the intrinsic dipole moment and the

[a]School of Chemical Engineering, University of Science and Technology Liaoning, Anshan 114051, China. E-mail: mkustl@163.com; zzhustl@163.com
[b]Sinochem LantianFluoro Materials Co., Ltd, China
[c]Oxiranchem Holding Group Co. Ltd, Liaoyang 111003, China
[d]Montverde Future Academy Shanghai, 88 jianhao Road, Pudong New District, Shanghai, 201318, China
[e]Department of Materials Science and Engineering, Cornell University, Ithaca, NY 14850, USA. E-mail: d.dastan61@yahoo.com

† Electronic supplementary information (ESI) available. See DOI: https://doi.org/10.1039/d2ra07043j

dipole polarization of polar functional groups lead to a significant increase in dielectric loss.[13] Therefore, the optimization of dielectric properties requires that the PI polymer chains contain non-polar functional groups.[14] In addition, the location of the polar functional groups is also significant. The polar group has a greater effect on the dielectric properties, if it is on the side chain of the polymer, especially on the flexible polar group with strong migration rate.[15,16] According to the Clausius–Mossotti formula,[17] the dielectric constant (D_K) of polymer dielectric materials can be expressed as follows:

$$(D_k - 1)/(D_k + 2) = P/V \quad (1)$$

where P ($cm^3\ mol^{-1}$) and V ($cm^3\ mol^{-1}$) are the molar polarization of polymer functional groups and the molar volume of polymer functional groups (free volume).

$$D_k = [1 + 2(P/V)]/[1 - (P/V)] \quad (2)$$

Based on these theoretical formulas, the lower the dielectric constant of the substrate, the lower the P/V value will be. The values of P and V, including –F, $-CH_3$, $-CH_2-$, $-C_6H_5$, –COO–, –CO–, –O– and –OH/$-C_6H_5$ are given in Table 1.[18] It is obvious that the introduction of –F, $-CH_2-$, $-CH_3$ groups can effectively reduce the D_k of polymer materials. The incorporation of fluorine atoms is a good way to reduce the dielectric constant of polymers. The consolidation of fluorine atoms is a good method to reduce the dielectric constant of PI polymers.[19] The fluorine atoms have the strongest electronegativity to fix the electrons, which makes the doping of fluorine atoms an effective strategy in reducing the polarizability of electrons and ions. Alternatively, the bond energy of C–F bond is strong and has a fluorine-containing group including a larger stereoselectivity.[20] Both the electron susceptibility and the dipole moments of the C–F bond are the lowest, making the fluoridation a selective preference for low dielectric constant applications.[21] However, the dielectric properties of these PIs need to be further increased to meet needs of the high frequency 5G communications applications. Therefore, it is of large importance to propose some methods to improve the dielectric properties, except molecular structure design.

Table 1 P and V values of common functional groups in polymers.[18]

Functional group	P/($cm^3\ mol^{-1}$)	V/($cm^3\ mol^{-1}$)
–F	1.8	10.9
$-CH_3$	5.6	23.9
$-CH_2-$	4.7	15.9
$-C_6H_5$	25.0	65.5
–COO–	15.0	23.0
–CO–	10.0	13.4
–O–	5.2	10.0
–OH, $-C_6H_5$	20.0	9.7

According to some literatures, host molecules of macrocyclic compounds and amino-containing guest molecules can form supramolecular host–guest envelops.[22–24] Self-assembly cooperation has proven to be effective in regulating the chemical structure and physical properties of polymer materials. Cyclodextrin can lower its dielectric constant through accommodating their own nano-morphology structure and cavity size for instance. As a host molecule similar to cyclodextrin, crown ethers (CEs) have smaller hollow structure and lower polarizability than cyclodextrin, and their ether bonds can lead to good dispersion.[25–28] With the presumption that the introduction of CEs might adjust PI macromolecule sinter chain packing structure and increase the polarization of PI molecular chain. It can be threaded by PI chains to construct necklace-like interlocking complexes *via* condensation polymerization.[25]

In this study, DB18-CE-6, one of the most common crown ethers, was employed as a host compound to prepare the complex of DB18-CE-6 and polyamic acid (PAA, the precursor of PI) with a necklace-like interlocking structure, which resulted in an DB18-CE-6-PI nanocomposite *via* thermal imidization. The dielectric constant, the dielectric loss, opticsand thermal properties of the composite PI films are evaluated in details. As a result, the dielectric constant of PI/CEs composite films are largely enhanced due to the introduction of CEs, although the optical transmittance and glass transition temperature relatively declined. Among the prepared samples, the PI-3/DB18CE-0.3 shows the lowest dielectric constant. Therefore, these CEs composites exhibit excellent dielectric properties, which are expected to be used in high frequency (10 GHz) 5G communications substrate in the future.

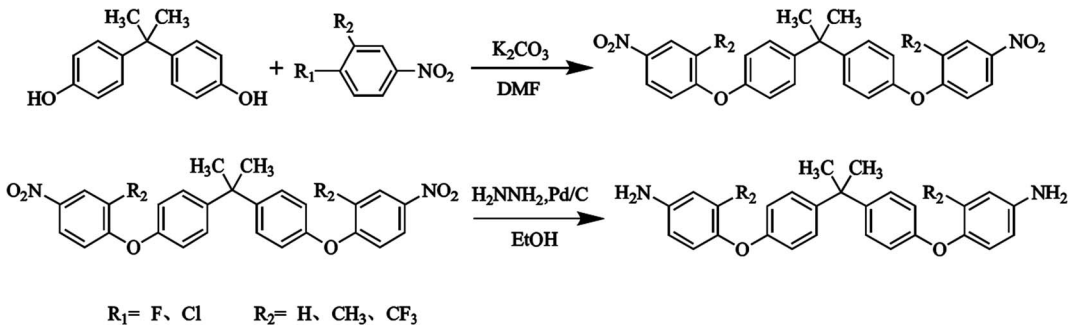

Scheme 1 Synthesis routes of the bisphenol A-containing diamines.

2. Experimental

2.1 Materials

The compound 2-fluoro 5-nitrotoluene (99%), 2-chloro-5-nitrotrifluoromethyl (98%), 1-chloro-4-nitrobenzene (99.5%), bisphenol A (99%), 4,4′-(hexafluoroisopropylidene)diphthalic anhydride(6FDA, 99%), DB18-CE-6 (98%), were purchased from Shanghai Aladdin Biochemical Technology Co., Ltd (China). Dianhydride was dried in vacuum at 125 °C for 24 h before samples preparation. All other reagents were obtained from Sinopharm Chemical Reagent Co., Ltd (China) and used as received.

2.2 Synthesis of the monomers

The synthesis steps of bisphenol A-containing diamines are shown in Scheme 1. The chemical structures were identified 1H NMR, as shown in Fig. S1.† Three kinds of diamine (BAPP, BAPP-2ME, BAPP-2TF) monomers with bisphenol A structure were synthesized respectively.

2.2.1 Synthesis of 2,2-bis[4-(4-nitrophenoxy)phenyl] propane (BNPP). Bisphenol A (23.060 g, 0.1 mol), anhydrous potassium carbonate (33.170 g, 0.24 mol) and *N*,*N*-dimethylformamide (DMF, 79.993 mL, 1.041 mol)were added to a 500 mL two-necked flask and kept stirring 2 h at 80 °C nitrogen protection and refluxed. Then, *p*-chloronitrobenzene (37.800 g, 0.24 mol) was introduced into the solution and heated to 140 °C. The reaction was refluxed and stirring for 6 h, and then obtained solution was suction filtered. The filter cake was repeatedly washed in room temperature until the obtain of colorless filtrate. 2,2-bis[4-(4-nitrophenoxy)phenyl]propane (BNPP) was obtained by recrystallization method according to the ratio of BNPP to DMF mass ratio of 1 : 1. The residue was recrystallized twice in DMF to obtain a shallow yellow mixed isomers powder (41.044 g).

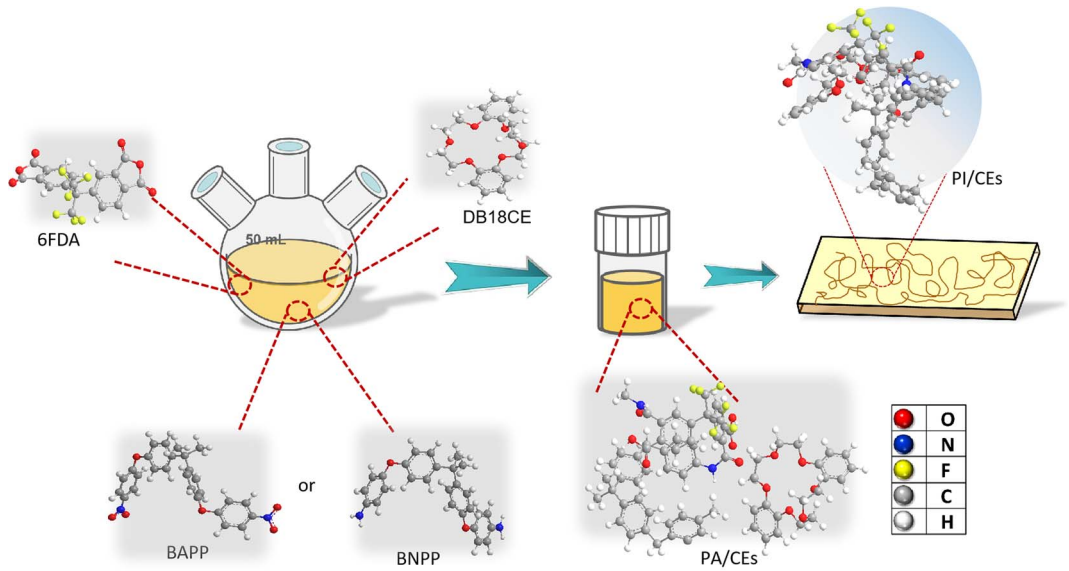

Fig. 1 Preparation of diamines, dianhydrides and PI/CEs film.

Table 2 Experimental formulation of polyimide films

System name	*n*(diamine)[a] (mmol)	*n*(DB18CE6)[a] (mmol)	*n*(6FDA)[a] (mmol)	*n*(DB18CE6)/*n*(6FAPB)[b]
PI-1	4.872	—	4.872	—
PI-1/0.1	4.872	0.487	4.872	0.1
PI-1/0.2	4.872	0.974	4.872	0.2
PI-1/0.3	4.872	1.462	4.872	0.3
PI-1/0.4	4.872	1.949	4.872	0.4
PI-2	4.872	—	4.872	—
PI-2/0.1	4.872	0.487	4.872	0.1
PI-2/0.2	4.872	0.974	4.872	0.2
PI-2/0.3	4.872	1.462	4.872	0.3
PI-2/0.4	4.872	1.949	4.872	0.4
PI-3	4.577	—	4.577	—
PI-3/0.1	4.577	0.458	4.577	0.1
PI-3/0.2	4.577	0.915	4.577	0.2
PI-3/0.3	4.577	1.373	4.577	0.3
PI-3/0.4	4.577	1.831	4.577	0.4

[a] The feed molar amount of BAPP/BAPP-2ME/BAPP-2TF, DB18CE6 and 6FDA. [b] The mole ratio of DB18CE6 to BAPP/BAPP-2ME/BAPP-2TF.

2.2.2 Synthesis of 2,2′-bis [4-(4-aminophenoxy)phenyl] propane(BAPP). The obtained BNPP (20.522 g, 0.044 mol), anhydrous ethanol (205.22 g), palladium/carbon (10%, 2.052 g) were added to 500 mL two-necked flask. The reaction was heated to 75 °C. Then, hydrazine hydrate (85%, 41.044 mL) was slowly added and the reaction was tracked by liquid chromatography (HPLC) for 5 h. A large amount of white crystal was precipitated, and the filter cake was washed in room temperature with ethanol repeatedly. Repeat the filter step and vacuum drying to obtain 2,2′-bis [4-(4-aminophenoxy)phenyl]propane(BAPP).The yield was about (17.033 g). According to similar method, other dinitro compounds and diamines were also synthesized.

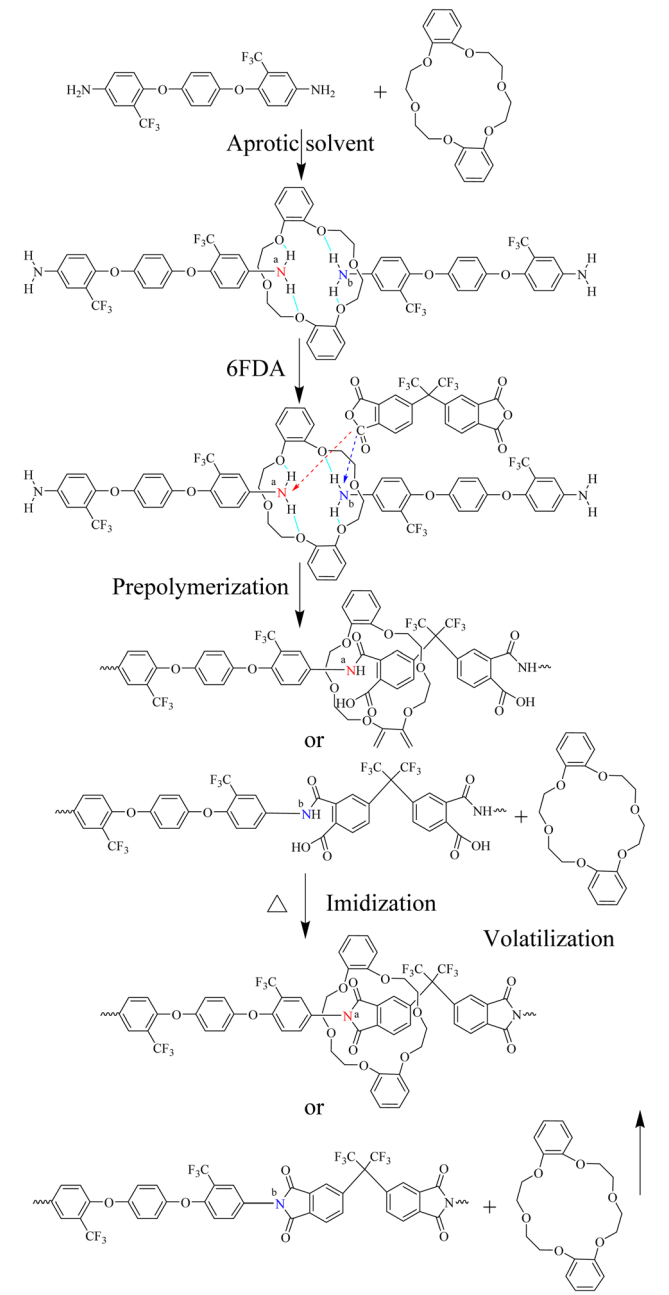

Scheme 2 The polymerization of diamines, dianhydrides, and CEs.

2.3 Preparation of DB18-CE-6-PI composite film

In this study, the molar ratio of diamine/dianhydride/crown ether was 1 : 1 : 0.1–0.4. The preparation procedure for composite films of PI/crown ether host–guest inclusion complex is illustrated in Fig. 1. The experimental formulation of PI films is shown in Table 2. The CEs was added before the PAA formation process. The MPI (modified polyimide films) were prepared according to the conventional two-step method,

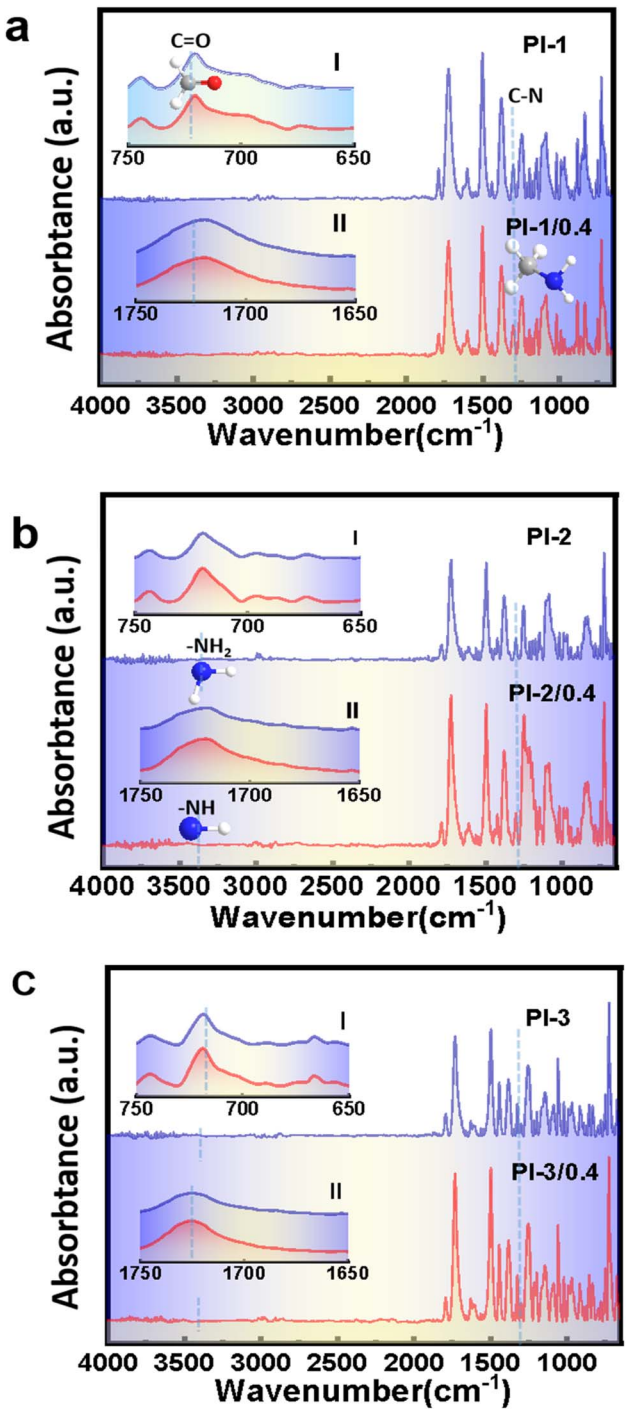

Fig. 2 FTIR spectra of PI/CEs composite films, (a) PI-1, PI-1/0.4, (b) PI-2, PI-2/0.4, (c) PI-3, PI-3/0.4.

including the solution polymerization of diamines and dianhydrides as well as thermal imidization, as shown in Scheme 2. First, 2.193 g (5.3 mol) of diamine BAPP and 10.248 g solvent *N*,*N*-dimethylacetamide (DMAc) were added to a 100 mL round bottom flask and stirred at a constant speed of 300 rpm until completely dissolved in room temperature. After the BAPP was completely dissolved, 2.089 g (4.7 mmol) of dianhydride 6FDA was introduced and continuously mixed at room temperature for 12 hours. Then, the obtained poly (amic acid) (PAA) solution was coated on a clean glass substrate, followed by the temperature-programmed thermal imidization, which was as follows: 80 °C per 10 min, 120 °C per 10 min, 170 °C per 20 min, 210 °C per 10 min, 250 °C per 10 min and 300 °C per 10 min. After natural cooling, the glass plate was immersed into a water bath at 80 °C to remove the film. Finally, the obtained film was dried at 100 °C for the next test.

2.4 Characterization

The chemical shifts of the dinitro compounds and diamines were measured by AVANCE 500 MHz nuclear magnetic field

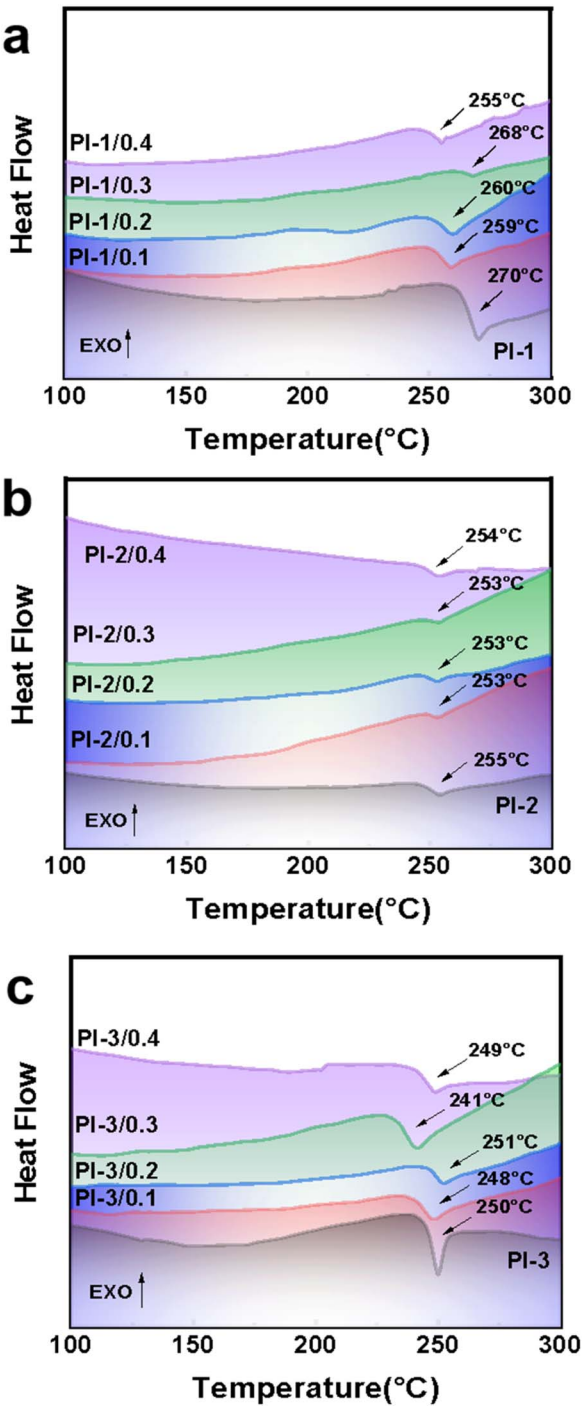

Fig. 3 DSC curves of PI/CEs composite films, (a) PI-1 series, (b) PI-2 series, (c) PI-3 series.

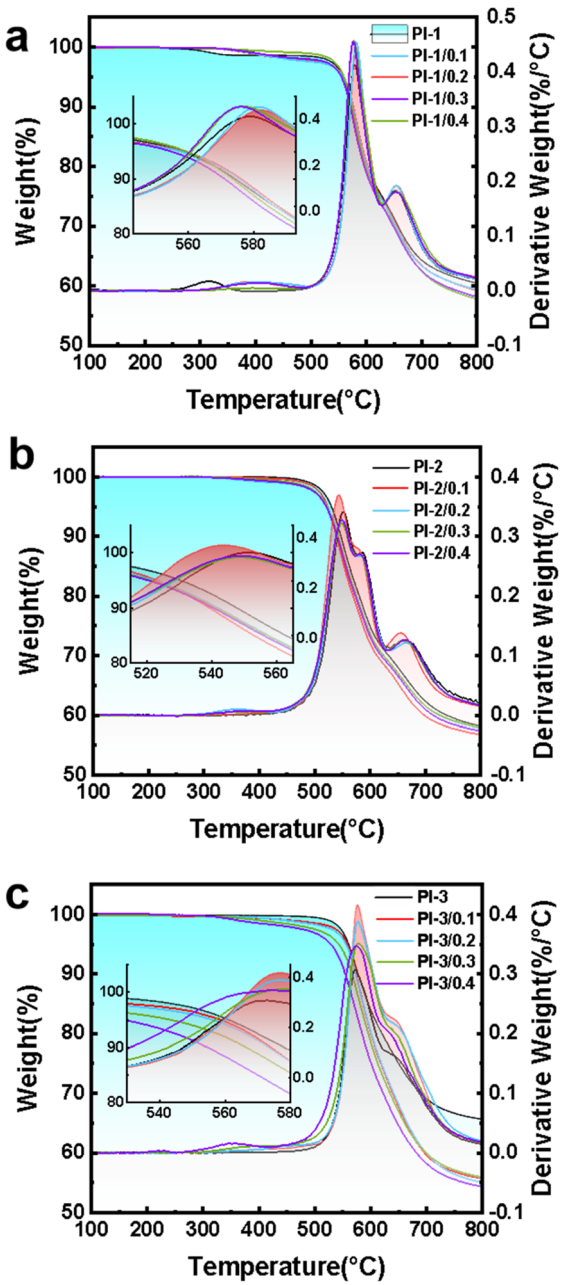

Fig. 4 TG-DTG curves of PI/CEs films, (a) PI-1 series, (b) PI-2 series, (c) PI-3 series.

resonator (Bruker, Swiss), and the deuterated reagent was dimethyl sulfoxide (DMSO). The characteristic functional groups of the compounds and polymers were tested by Nicolet IS10 Fourier infrared spectrometer (Thermo Fisher Scientific,USA) in the range of 500–4000 cm^{-1}. Pyris 1 TGA thermal analyzer (PerkinElemer, USA) was used to investigate the thermal stabilities of the polyimides, with a heating rate of 20 °C min^{-1} and nitrogen flow rate of 20 mL min^{-1} in the range of 30–600 °C. Based on the maximum tan δ peak, the glass transition temperature (T_g) of the polyimides was determined. The UV-visible absorption spectra of the film samples were tested by Lambda 900 UV/Vis/NIR spectrophotometer (PerkinElmer, USA), scanning from 250 to 800 nm. The dielectric constant and dielectric loss of polyimide film were tested by the AET (high frequency cavity resonator) microwave (high-frequency 10 GHz) dielectric constant tester (AET Corporation, Japan), with the sample size of 10 cm × 1 cm. The samples were tested by Guilin Saimeng Testing Technology Co., Ltd.

3. Results and discussions

3.1 Chemical structures

The chemical structures of crown ether-containing polyimides were identified by FTIR, as shown in Fig. 2. It can be seen that the three pristine polyimides exhibit characteristic peaks of imide ring, including 1786 cm^{-1} (the asymmetric stretching vibration peak of C═O group), 1722 cm^{-1} (the symmetric stretching vibration peak of C═O group) and 1375 cm^{-1} (the stretching vibration absorption of C–N bond), 716 cm^{-1} (out-of-plane C═O bending motion). Meanwhile, the characteristic peaks of $-NH_2$ at 3400.03 cm^{-1} and –N–H at 3331.57 cm^{-1} do not appear. This guarantees that poly (amic acid) (PAA) has been totally thermal-cured to PI. These characteristic peaks indicate that the polyimides have undergone a relatively complete imidization process.[29,30]

By contrast, as shown in Fig. 2, the original characteristic peaks PI-1 of C═O at 720 and 1719 cm^{-1} demonstrate a shift to 716 and 1721 cm^{-1}, respectively. The same situation is also observed for PI-2-18-crown ether-6 and PI-3-18-crown ether-6 films.[31,32] These results are consistent with those reported in literature,[33–36] which confirm the inclusion complex structure formed between PI macro-molecules and CEs molecules.

3.2 Thermal properties

The thermal properties of PI/CEs films are evaluated by DSC (in Fig. 3) and TG-DTG (in Fig. 4), and the corresponding data are listed in Table 3. DSC curves are used to investigate the thermal

Table 3 Thermal data of PI/CEs composite films

Samples	T_g (°C)	T_{d5} (°C)	T_{d10} (°C)	RW750
PI-1	270	559.85	575.72	61.86
PI-1/0.1	259	558.37	576.25	60.79
PI-1/0.2	260	557.75	575.62	60.82
PI-1/0.3	268	559.22	573.60	59.39
PI-1/0.4	255	554.74	571.11	59.71
PI-2	253	530.52	547.88	59.58
PI-2/0.1	253	521.46	541.49	59.15
PI-2/0.2	253	522.66	542.20	59.04
PI-2/0.3	253	520.71	540.60	58.49
PI-2/0.4	254	523.35	539.39	57.79
PI-3	250	560.91	577.90	66.66
PI-3/0.1	248	560.25	577.23	56.80
PI-3/0.2	251	551.28	565.96	57.14
PI-3/0.3	241	551.07	571.96	56.31
PI-3/0.4	249	558.36	574.94	56.59

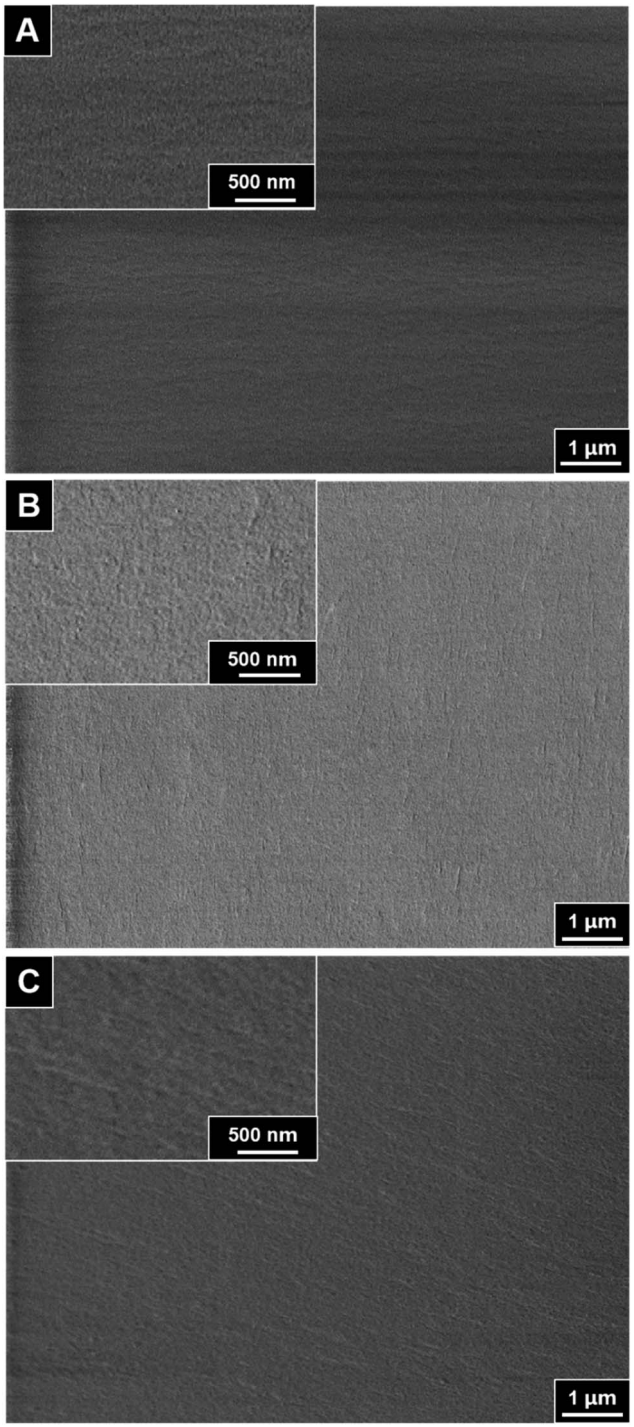

Fig. 5 SEM images of PI origin films cross-section (A) PI-1, (B) PI-2, (C) PI-3.

stability of the prepared PI films are (Fig. 3), and the results are listed in Table 3. Tg values of the PI films are at about 250 °C. This is mainly because the main structures of the PIs polymer molecular chains are similar. By comparison, the trifluoromethyl exhibit the lowest T_g than no side-chain groups PIs and methyl side-chain groups PI, which is ascribed to the highest steric hindrance of trifluoromethyls. The large steric hindrance causes intermolecular forces decreasing, and makes the molecular thermal motion be easier, which is resulted in a decrease in T_g values.[37,38] Since crown ether is a macromolecular cyclic substance, the PI polymer chains are more likely to slip after doping with crown ether, which is resulted in a slight decrease in T_g values.[39,40]

To fully evaluate the thermal properties of polyimides, TG-DTG were carried out to estimate the thermal properties, and the obtained curves are shown in Fig. 4. The corresponding data are summarized in Table 3. As shown in Fig. 4, the TG-DTG curves of PI-CEs films show extremely similar weight loss. These films exhibit a main weight loss at above 520 °C. The PI films based on three different kinds of bisphenol A diamine monomers in combination with 6FDA show high thermal stability and their residual carbon rates are above 56%. The bisphenol A-based polyimides display higher thermal decomposition temperatures than the alicyclic polyimides because of the strong stabilization of aromatic structures. Due to the thermal instability of $-CH_3$ substituent groups on the PI-2 films, the thermal decomposition temperature T_{d5} and T_{d10} are relatively lower. However, the PI-3 series have similar thermal decomposition temperatures with PI-1 series, which is mostly ascribed to the space effect of $-CF_3$ steric hindrance and instability of substituent groups that can cancel each other out. By comparison, the CE-0.1 MPIs exhibit resemble thermal decomposition temperatures with the original PIs, which is ascribed to the PI molecular chains that are fully wrapped around the crown ether. The crown ethers are well fused with the PI films. The CEs molecules are not easy to volatilize from PI films when the films are heated. However, with the increase of doping amount, the CE-0.4 MPIs display lower thermal decomposition temperatures.[41,42]

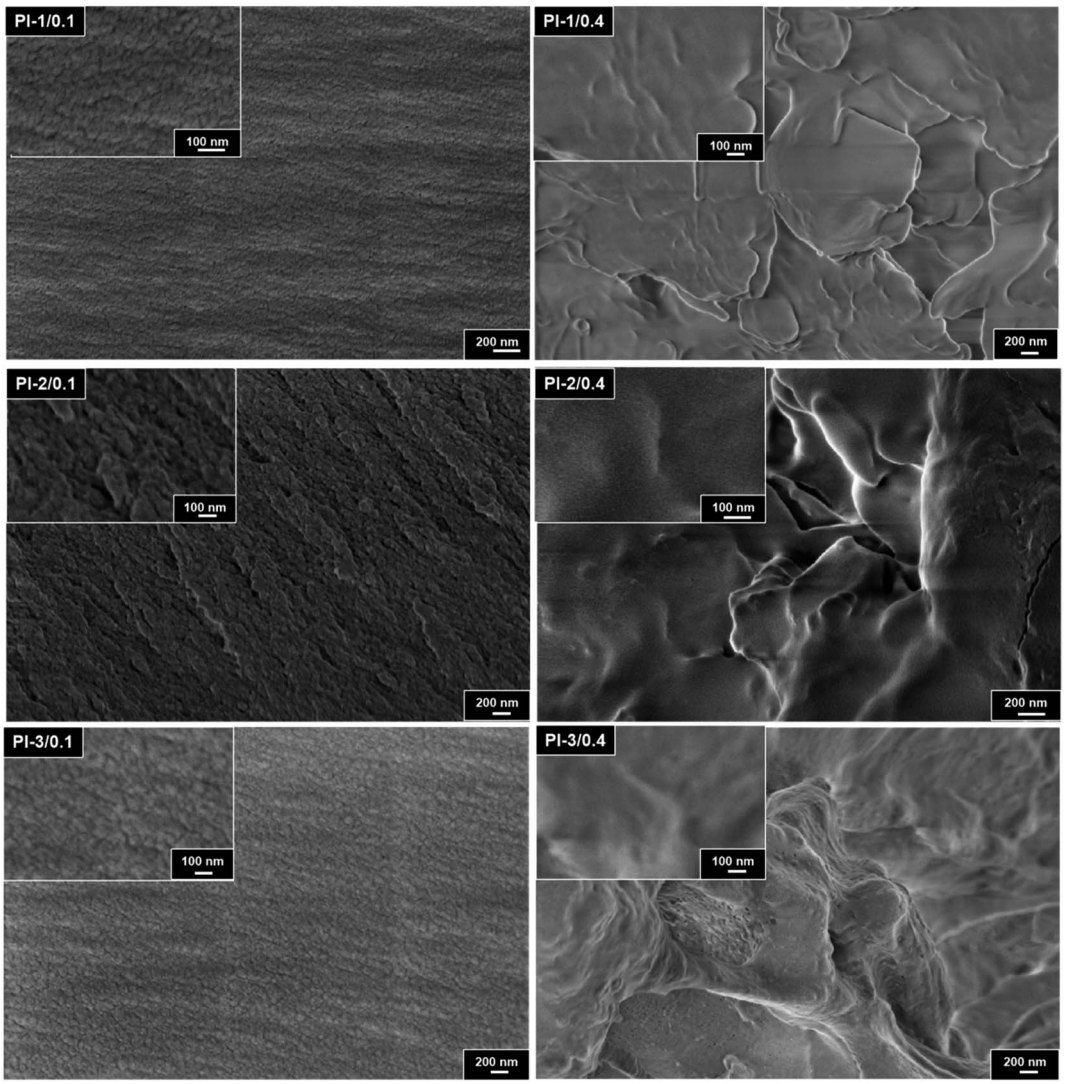

Fig. 6 SEM images of PI origin films cross-section.

Due to the fact that CEs cannot be fully wrapped by the PI molecular chains, the thermal decomposition temperature $T_{d5}$and T_{d10} of CE-0.4 MPIs are relatively lower.

3.3 Membrane morphology

Scanning electron microscopy was employed to compare the cross-section morphology of three origin PI film (three kinds of bisphenol A diamine monomers in combination with 6FDA directly) and the crown ether addition MPI (modified polyimide) films. The differences between membranes cross-section morphology with crown ether addition and no addition are noticeable.

In Fig. 5, the cross-section of three pristine polyimides films without crown ether addition are smooth and dense, and no holes and defects are observed. It indicates that the obtained polyimides have high molecular weight and the monomers have high reactivity. The cross-section of PI gradually transitioned from smooth to rough with crown ether addition process. The SEM images illustrate that the cross-section of PI composite films are not uniform and contained cracks with scaly appearance, which indicates that the films are ductile fracture.[43,44] In Fig. 6, the section roughness of PI composite films gradually increases with the increase of crown ether doping amount from 0.1 to 0.4 mol. This is mainly due to the molecular chains of MPIs which are more prone to slip under the stress condition. Compared with PI-2 and PI-3 series, the PI-1 series MPI cross-sectional morphology are slightly more regular, which is attributed to the diamine monomers that are free of contain pendant groups and the fact that the free volume of the polymer chains is smaller.

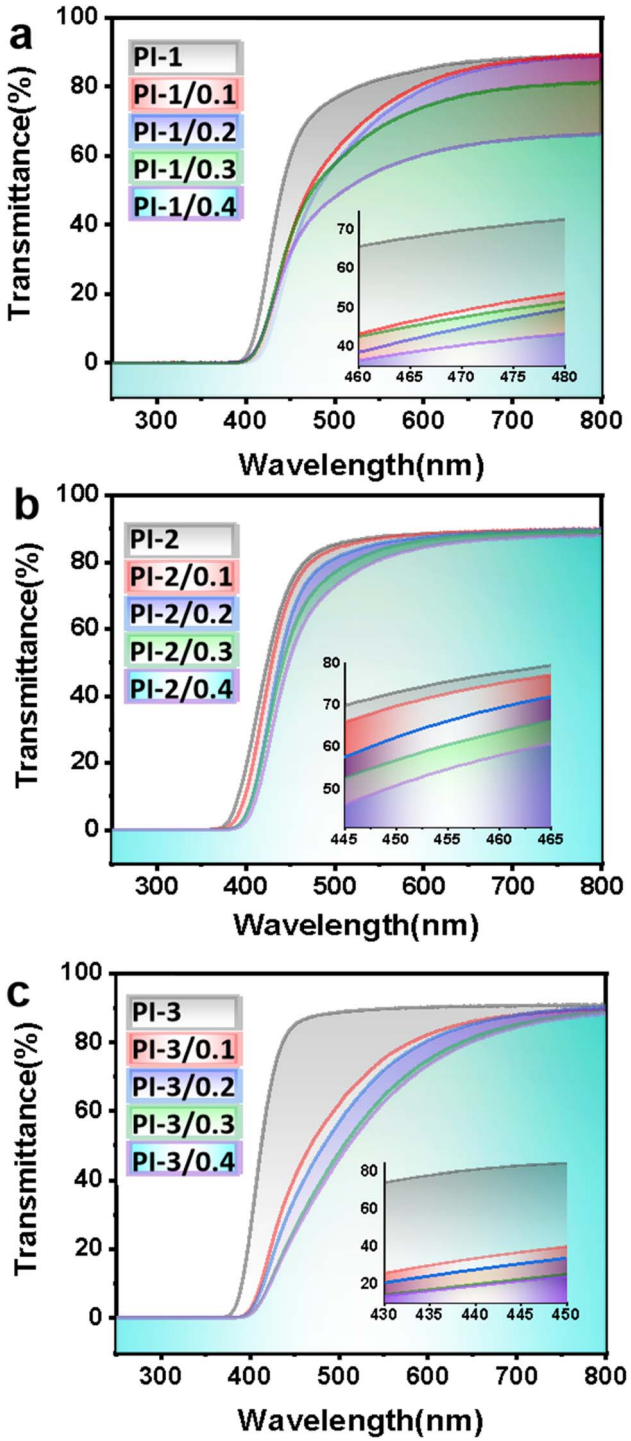

Fig. 7 UV-visible spectra of PI/CEs films, (a) PI-1, (b) PI-2, (c) PI-3.

3.4 Optical properties

The UV-visible spectra as well as the data of optical properties are shown in Fig. 7 and Table 4. It can be observed that the shortest UV cut-off wavelength of 364–398 nm, and their optical transparency are 30.28–80.70% at 450 nm. The cut-off wavelengths are similar since the dianhydride monomers of the three films are the same bisphenol A structure. The semblable molecular structure of the films makes no obvious difference in the absorption of ultraviolet light. However, the introduction of different side chain groups causes biggish discrepancies of electrons transfer in the polymer chains. The results of optical properties show a better transparency for PI-3 films compared to other samples, which are probably caused by the steric hindrance effect of $-CF_3$ groups to further increase the distance

Table 4 Optical data of PI/CEs films

Samples	Cut-off wavelength (nm)	Transmittance at 450 nm (%)
PI-1	385	59.17
PI-1/0.1	393	45.45
PI-1/0.2	398	40.28
PI-1/0.3	388	35.88
PI-1/0.4	386	31.25
PI-2	358	72.84
PI-2/0.1	364	69.76
PI-2/0.2	374	62.42
PI-2/0.3	372	56.79
PI-2/0.4	379	50.78
PI-3	366	84.70
PI-3/0.1	365	67.38
PI-3/0.2	379	50.29
PI-3/0.3	379	44.06
PI-3/0.4	368	42.63

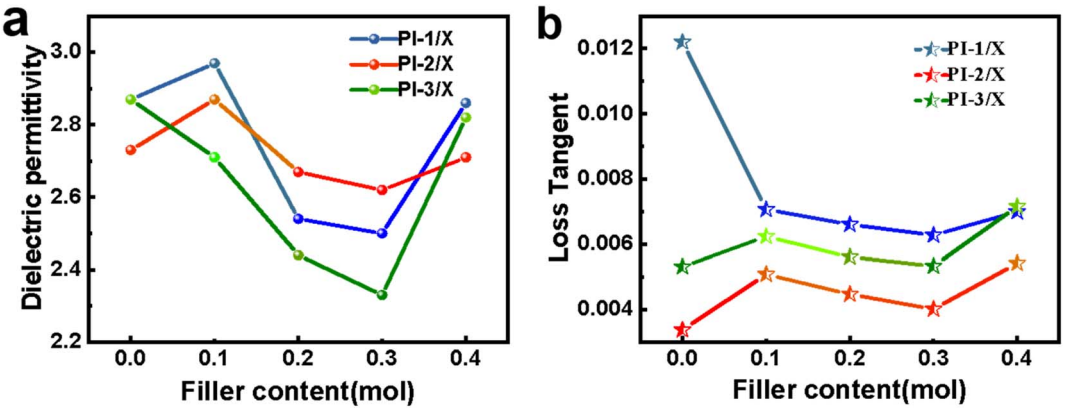

Fig. 8 Dielectric constant (a) and dielectric loss (b) of PI/CEs films.

between molecular chains and hinder the formation of CTCs (charge transfer complexes). With the increase of crown ether amount, the optical transparency at 450 nm of PI-1 films reduce from 59.17% to about 30%, the PI-2 films reduce from 72.84% to 50.78%, and the PI-3 films reduce from 84.70% to 42.63%. The decrease of optical transparency is mainly due to the introduction of crown ethers which reduces the crystallinity of polymers. The crown ether was uniformly dispersed in PAA solution and the polymers were formed by polycondensation. The interspersion of macromolecular cyclic compounds could weaken the free movement of molecular chains and reduce the crystallinity of polymers. Because a secondary wave light, which is inconsistent with the main wave, is generated when light propagates between the crystalline phase and the amorphous phase. The secondary wave interferes with the main wave and occurs scattering phenomenon. The intensity of transmitted light reduces which is mostly ascribed to the main wave deviation.

3.5 Dielectric properties

Depending on the chemical structures, PIs possess different dielectric constant. The dielectric performance of polyimide was tested at 10 GHz and the volt–ampere diagram is shown in Fig. 8. The dielectric data of the polyimides are shown in Table 5. Because of the strong electron absorption and large free volume, the $-CF_3$ group is considered to be an effective way to reduce the dielectric constant. It can be seen that all prepared MPI films showed dielectric constants below 3.0, meeting the need of the high-frequency communication substrates.

A downward trend and then an upward trend at dielectric constants are observed as the crown ether doping amounts increases. This is mainly due to the fact that when the content of crown ether is low, the molecular chain evenly wraps the cyclic macromolecular crown ether, which increases the free volume of the matrix and reduces the dielectric constant of the film. The dielectric constant is higher, which is possibly due to the PI molecular chains evenly wrapped the cyclic macromolecular crown ether at a low crown ether content.[45] The free volume of the matrix is increased and the dielectric constant is reduced.[46] The PI-1films shows the highest dielectric loss and PI-2 films exhibit the lowest dielectric loss.[47–49] Because the addition of $-CH_3$ pendant group of PI-2 films increases the imbalance of PI molecular chain, the imbalance of PI molecular chain is increased, and the reactivity is increased through the addition of electron donating $-CH_3$ group. The degree of polymerization is increased, which resulted in a decrease of end groups in per unit volume. Consequently, the dielectric loss reduction of PI-2 films is the most obvious one. The increased $-CF_3$pendant group of PI-3 films exhibit a minor reduction of the dielectric loss because the two bulky polar $-CF_3$ groups of 6FDA recede the Felement influence.[50–52]

Table 5 Dielectric properties of PI/CEs films

Samples	Dielectric constant	Dielectric loss
PI-1	2.87	0.01220
PI-1/0.1	2.97	0.00707
PI-1/0.2	2.54	0.00661
PI-1/0.3	2.50	0.00628
PI-1/0.4	2.86	0.00700
PI-2	2.73	0.00337
PI-2/0.1	2.87	0.00508
PI-2/0.2	2.67	0.00447
PI-2/0.3	2.62	0.00401
PI-2/0.4	2.71	0.00542
PI-3	2.87	0.00531
PI-3/0.1	2.71	0.00624
PI-3/0.2	2.44	0.00561
PI-3/0.3	2.33	0.00533
PI-3/0.4	2.82	0.00716

4. Conclusion

Three kinds of bisphenol A diamine monomers are effectively synthesized, and the corresponding polyimide films are modified with DB18-CE-6, according to the two-step method. The diamine BAPP, BAPP-2ME (containing methyls) and BAPP-2TF (trifluoromethyls) are synthesized and polymerized with 6FDA (fluorine) to prepare the low dielectric constant and low dielectric loss PI films. By virtue of *in situ* polymerization, DB18-CE-6 is introduced into the PI (BAPP-6FDA) matrix to fabricate

the corresponding trifluoromethyls composite films. These films show excellent dielectric properties. The 2TF films exhibit the lowest Tg than no side-chain groups PIs and the 2ME films, which is ascribed to the highest steric hindrance of trifluoromethyls. With an increase in the CEs content, the T_g of CEs composite film decreases slightly, while the thermal decomposition temperature exhibits a decline trend. A small amount of DB18-CE-6 doping has no obvious effect on the thermal stability of the MPI films, which is ascribed to the fact that PI molecular chains are fully wrapped around the crown ether. Particularly, all these modified polyimide films exhibit good dielectric properties with dielectric constants below 3.0, and the 2TF films show the lowest dielectric loss. The lowest-dielectric constant (low-k) films have been prepared by n(Crown ether)/n(6FAPB) = 0.3, the PI-1 films tan δ decreases from 0.01220 to 0.00628, with a decrease rate of 48.52%. Therefore, this paper reports a simple method to reduce the dielectric constant and dielectric loss of PI films containing different side groups by introducing CEs.

In mostly literature, the dielectric constant and loss are generally tested at low frequencies (1 MHz). However, in this paper, the dielectric constant and loss were tested at high frequencies (10 GHz) and the minimum dielectric constant can be low to 2.33. In Chuqi Shi[10] and Ruxin Bei[47] results, the dielectric constants are 2.50 and 2.44 respectively. Compared with the 2.33 dielectric constant obtained from this study, our data is relatively better. In theory, the smaller the dielectric constant and loss are, the better and clearer the signal can be got.

In addition, the synthesis process is more simple and cost lower in this experiment. The addition of crown ether can reduce the dielectric constant by 18.82%, and the dielectric loss to 72.38%. The reagents and catalysts in this experiment can be recycled. These modified PI films are expected to be used in high frequency (10 GHz) 5G communications substrate.

Conflicts of interest

There are no conflicts to declare.

Acknowledgements

This work were financially supported by the Education Department of Liaoning Province (LJKMZ20220660), and the University of Science and Technology Liaoning Talent Project Grants (grant number: 2020QN05 and 601010403).

References

1 L. Wang, J. Yang, W. Cheng, J. Zou and D. Zhao, Progress on Polymer Composites With Low Dielectric Constant and Low Dielectric Loss for High-Frequency Signal Transmission, *Front. Mater.*, 2021, **8**, 434.

2 D.-J. Liaw, K.-L. Wang, Y.-C. Huang, K.-R. Lee, J.-Y. Lai and C.-S. Ha, Advanced polyimide materials: Syntheses, physical properties and applications, *Prog. Polym. Sci.*, 2012, **37**, 907–974.

3 J. Huang, X. Li, L. Luo, H. Wang, X. Wang, K. Li, C. Zhang and X. Liu, Releasing silica-confined macromolecular crystallization to enhance mechanical properties of polyimide/silica hybrid fibers, *Compos. Sci. Technol.*, 2014, **101**, 24–31.

4 B. G. Kim, Y. S. Kim, Y. H. Kim, H. Kim, Y. J. Hong, H. M. Jung and J. C. Won, Nano-scale insulation effect of polypyrrole/polyimide core–shell nanoparticles for dielectric composites, *Compos. Sci. Technol.*, 2016, **129**, 153–159.

5 P. Liu, T. Q. Tran, Z. Fan and H. M. Duong, Formation mechanisms and morphological effects on multi-properties of carbon nanotube fibers and their polyimide aerogel-coated composites, *Compos. Sci. Technol.*, 2015, **117**, 114–120.

6 K. Wang, K. Amin, Z. An, Z. Cai, H. Chen, H. Chen, Y. Dong, X. Feng, W. Fu and J. Gu, Advanced functional polymer materials, *Mater. Chem. Front.*, 2020, **4**, 1803–1915.

7 O. A. Tafreshi, S. Ghaffari-Mosanenzadeh, S. Karamikamkar, Z. Saadatnia, S. Kiddell, C. B. Park and H. E. Naguib, Novel, flexible, and transparent thin film polyimide aerogels with enhanced thermal insulation and high service temperature, *J. Mater. Chem. C*, 2022, **10**, 5088–5108.

8 C.-K. Min, T.-B. Wu, W.-T. Yang and C.-L. Chen, Functionalized mesoporous silica/polyimide nanocomposite thin films with improved mechanical properties and low dielectric constant, *Compos. Sci. Technol.*, 2008, **68**, 1570–1578.

9 Y. Liu, C. Qian, L. Qu, Y. Wu, Y. Zhang, X. Wu, B. Zou, W. Chen, Z. Chen, Z. Chi, S. Liu, X. Chen and J. Xu, A Bulk Dielectric Polymer Film with Intrinsic Ultralow Dielectric Constant and Outstanding Comprehensive Properties, *Chem. Mater.*, 2015, **27**, 6543–6549.

10 C. Shi, S. Liu, Y. Li, Y. Yuan, J. Zhao and Y. Fu, Imparting low dielectric constant and high modulus to polyimides via synergy between coupled silsesquioxanes and crown ethers, *Compos. Sci. Technol.*, 2017, **142**, 117–123.

11 S. Chisca, V. E. Musteata, I. Sava and M. Bruma, Dielectric behavior of some aromatic polyimide films, *Eur. Polym. J.*, 2011, **47**, 1186–1197.

12 Y. Watanabe, Y. Shibasaki, S. Ando and M. Ueda, Synthesis and Characterization of Novel Low-k Polyimides from Aromatic Dianhydrides and Aromatic Diamine Containing Phenylene Ether and Perfluorobiphenyl Units, *Polym. J.*, 2006, **38**, 79–84.

13 S. Bonardd, V. Moreno-Serna, G. Kortaberria, D. Diaz Diaz, A. Leiva and C. Saldias, Dipolar Glass Polymers Containing Polarizable Groups as Dielectric Materials for Energy Storage Application, A Minireview, *Polymers*, 2019, 11.

14 Z. Hu, X. Liu, T. Ren, H. A. Saeed, Q. Wang, X. Cui, K. Huai, S. Huang, Y. Xia and K. K. Fu, Research progress of low dielectric constant polymer materials, *J. Polym. Eng.*, 2022, **42**, 677–687.

15 B. Xu, X. Yi, T. Y. Huang, Z. Zheng, J. Zhang, A. Salehi, V. Coropceanu, C. H. Y. Ho, S. R. Marder, M. F. Toney, J. L. Brédas, F. So and J. R. Reynolds, Donor Conjugated Polymers with Polar Side Chain Groups: The Role of

Dielectric Constant and Energetic Disorder on Photovoltaic Performance, *Adv. Funct. Mater.*, 2018, **28**(46), 1803418.

16 Y. Oshiro, M. Miyasaka, Y. Shirota and H. Mikawa, Synthesis of the Polymer with Polar Side Groups. II. Synthesis and Dielectric Properties of the β-Cyanopropionaldehyde Acetal of Poly (vinyl alcohol), *Polym. J.*, 1974, **6**, 12–19.

17 G. Hougham, G. Tesoro, A. Viehbeck and J. Chapple-Sokol, Polarization effects of fluorine on the relative permittivity in polyimides, *Macromolecules*, 1994, **27**, 5964–5971.

18 G. Maier, Low dielectric constant polymers for microelectronics, *Prog. Polym. Sci.*, 2001, **26**, 3–65.

19 Y. Liu, P. Guo, P. Gao, J. Tong, J. Li, E. Wang, C. Wang and Y. Xia, Effect of fluorine atoms on optoelectronic, aggregation and dielectric constants of 2,1,3-benzothiadiazole-based alternating conjugated polymers, *Dyes Pigm.*, 2021, **193**, 109486.

20 M. G. Dhara and S. Banerjee, Fluorinated high-performance polymers: Poly(arylene ether)s and aromatic polyimides containing trifluoromethyl groups, *Prog. Polym. Sci.*, 2010, **35**, 1022–1077.

21 Q. Yang, Z. Chi, Q. Li and S. Scheiner, Effect of carbon hybridization in C-F bond as an electron donor in triel bonds, *J. Chem. Phys.*, 2020, **153**, 074304.

22 G. Chen and M. Jiang, Cyclodextrin-based inclusion complexation bridging supramolecular chemistry and macromolecular self-assembly, *Chem. Soc. Rev.*, 2011, **40**, 2254–2266.

23 M. Guo and M. Jiang, Macromolecular self-assembly based on inclusion complexation of cyclodextrins, *Prog. Chem.*, 2007, **19**, 557.

24 J. W. Steed, D. R. Turner and K. J. Wallace, *Core concepts in supramolecular chemistry and nanochemistry*, Wiley, 2007.

25 Y. Li, J. Q. Zhao, Y. C. Yuan, C. Q. Shi, S. M. Liu, S. J. Yan, Y. Zhao and M. Q. Zhang, Polyimide/Crown Ether Composite Films with Necklace-Like Supramolecular Structure and Improved Mechanical, Dielectric, and Hydrophobic Properties, *Macromolecules*, 2015, **48**, 2173–2183.

26 L. Yang, Y. Kang, Y. Wang, L. Xu, H. Kita, K. I. Okamoto, L. Yang, Y. Kang, Y. Wang, L. Xu, H. Kita and K. Okamoto, Synthesis of crown ether-containing copolyimides and their pervaporation properties to benzene/cyclohexane mixtures, *J. Membr. Sci.*, 2005, **249**, 33–39.

27 S.-H. Kim, C.-W. Lee, Y.-M. Jeon and M.-S. Gong, Synthesis and properties of calix [4] crown-6 functionalized polymers, *Macromol. Res.*, 2005, **13**, 141–146.

28 S. H. Chan, W. T. Wong and W. K. Chan, Synthesis and properties of polyimide with diazacrown ether moiety and the corresponding polymer barium complexes, *Chem. Mater.*, 2001, **13**, 4635–4641.

29 W. Bai, Z. Hu, Y. Lu, G. Xiao, H. Zhao, J. Zhu and Z. Liu, Solubility, thermal and photoluminescence properties of triphenyl imidazole-containing polyimides, *RSC Adv.*, 2021, **11**, 23802–23814.

30 W. Bai, Y. Lu, Z. Hu, G. Xiao, H. Zhao, J. Zhu and Z. Liu, Photoluminescence, thermal and surface properties of triarylimidazole-containing polyimide nanocomposite films, *RSC Adv.*, 2021, **11**, 36066–36077.

31 Y. Lu, J. Hao, G. Xiao, H. Zhao, Z. Hu and T. Wang, In situ polymerization and performance of alicyclic polyimide/graphene oxide nanocomposites derived from 6FAPB and CBDA, *Appl. Surf. Sci.*, 2017, **394**, 78–86.

32 Y. Lu, J. Hao, G. Xiao, L. Chen, T. Wang and Z. Hu, Preparation and properties of in situ amino-functionalized graphene oxide/polyimide composite films, *Appl. Surf. Sci.*, 2017, **422**, 710–719.

33 Z. Liu, H. Zhang and J. Han, Crown ether–pillararene hybrid macrocyclic systems, *Org. Biomol. Chem.*, 2021, **19**, 3287–3302.

34 R. Ikura, J. Park, M. Osaki, H. Yamaguchi, A. Harada and Y. Takashima, Design of self-healing and self-restoring materials utilizing reversible and movable crosslinks, *NPG Asia Mater.*, 2022, **14**, 1–17.

35 F. Nicoli, M. Baroncini, S. Silvi, J. Groppi and A. Credi, Direct synthetic routes to functionalised crown ethers, *Org. Chem. Front.*, 2021, **8**, 5531–5549.

36 S. Liu, Q. Feng, Y. Li, Z. Chen and J. Zhao, Simultaneously Improving Dielectric and Mechanical Properties of Crown Ether/Fluorinated Polyimide Films with Necklace-Like Supramolecular Structure, *Macromol. Chem. Phys.*, 2020, **221**, 2000256.

37 Y. Liu, G. Shi and G. Wu, Tuning the dynamic fragility of acrylic polymers by small molecules: the interplay of molecular structures, *Soft Matter*, 2021, **17**, 7541–7553.

38 D. W. Van Krevelen and K. Te Nijenhuis, *Properties of polymers: Their correlation with chemical structure; their numerical estimation and prediction from additive group contributions*, Elsevier, 2009, pp. 20091–21004.

39 B. Deng, S. Zhang, C. Liu, W. Li, X. Zhang, H. Wei and C. Gong, Synthesis and properties of soluble aromatic polyimides from novel 4, 5-diazafluorene-containing dianhydride, *RSC Adv.*, 2018, **8**, 194–205.

40 Y. Li, T. Chen, Y. Liu, X. Liu and X. Wang, Simultaneously enhance dielectric strength and reduce dielectric loss of polyimide by compositing reactive fluorinated graphene filler, *Polymer*, 2022, 125084.

41 Y. Liu, Z. Zhou, L. Qu, B. Zou, Z. Chen, Y. Zhang, S. Liu, Z. Chi, X. Chen and J. Xu, Exceptionally thermostable and soluble aromatic polyimides with special characteristics: intrinsic ultralow dielectric constant, static random access memory behaviors, transparency and fluorescence, *Mater. Chem. Front.*, 2017, **1**, 326–337.

42 X. Liu, J. Zhou, Y. Zhou, M. Wu, Y. Zhu, J. Zhao, S. Liu and H. Xiao, Chemically crosslinked polyimide-POSS hybrid: a dielectric material with improved dimensional stability and dielectric properties, *Eur. Polym. J.*, 2022, 111315.

43 J. A. Hinkley and S. Mings, Fracture toughness of polyimide films, *Polymer*, 1990, **31**, 75–77.

44 L. An, Y. Pan, X. Shen, H. Lu and Y. Yang, Rod-like attapulgite/polyimide nanocomposites with simultaneously improved strength, toughness, thermal stability and related mechanisms, *J. Mater. Chem.*, 2008, **18**, 4928–4941.

45 T. Zhu, C. Qian, W. Zheng, R. Bei, S. Liu, Z. Chi, X. Chen, Y. Zhang and J. Xu, Modified halloysite nanotube filled polyimide composites for film capacitors: high dielectric constant, low dielectric loss and excellent heat resistance, *RSC Adv.*, 2018, **8**, 10522–10531.

46 Y.-H. Chou, H.-J. Yen, C.-L. Tsai, W.-Y. Lee, G.-S. Liou and W.-C. Chen, Nonvolatile transistor memory devices using high dielectric constant polyimide electrets, *J. Mater. Chem. C*, 2013, **1**, 3235–3243.

47 R. Bei, C. Qian, Y. Zhang, Z. Chi, S. Liu, X. Chen, J. Xu and M. P. Aldred, Intrinsic low dielectric constant polyimides: relationship between molecular structure and dielectric properties, *J. Mater. Chem. C*, 2017, **5**, 12807–12815.

48 X. Peng, W. Xu, L. Chen, Y. Ding, S. Chen, X. Wang and H. Hou, Polyimide complexes with high dielectric performance: Toward polymer film capacitor applications, *J. Mater. Chem. C*, 2016, **4**, 6452–6456.

49 W. Peng, H. Lei, L. Qiu, F. Bao and M. Huang, Perfluorocyclobutyl-containing transparent polyimides with low dielectric constant and low dielectric loss, *Polym. Chem.*, 2022, **13**, 3949–3955.

50 J. Zhou, Y. Tao, X. Chen, X. Chen, L. Fang, Y. Wang, J. Sun and Q. Fang, Perfluorocyclobutyl-based polymers for functional materials, *Mater. Chem. Front.*, 2019, **3**, 1280–1301.

51 D. Dastan, K. Shan, T. Marszalek, M. K. A. Mohammed, L. Tao, Z. Shi, Y. Chen, X.-T. Yin, N. D. Alharbi, F. Gity, S. Asgary, M. Hatamvand and L. Ansari, Influence of heat treatment on H_2S gas sensing features of NiO thin films deposited *via* thermal evaporation technique, *Mater. Sci. Semicond. Process.*, 2023, **154**, 107232.

52 L. Tao, D. Dastan, W. Wang, P. Poldorn, X. Meng, M. Wu, H. Zhao, H. Zhang, L. Li and B. An, Metal-decorated InN monolayer senses N_2 against CO_2, *ACS Appl. Mater. Interfaces*, 2023, DOI: **10.1021/acsami.2c21463**.